

Unsteady Viscous-Inviscid Coupling Simulations of Separated Laminar Flows Around 2D Airfoils

José I. Rothkegel and Grigorios Dimitriadis

Aerospace and Mechanical Engineering Department

Chemin des Chevreuils 1, 4000, Liège, Belgium

Keywords: separated flow, boundary layer, finite volume, panel method, double wake, vortex blob

Abstract: An interactive boundary layer model has been developed in 2D in order to solve the unsteady flow around an airfoil. The inviscid problem is solved using a panel method, by the discretization of the airfoil into linear-varying vortex panels. The solution of the boundary layer equations is carried out using a finite volume scheme. Viscous-inviscid coupling is performed by imposing a permeation velocity on the skin panels of the airfoil and the addition of a free wake at each separation point.

1 INTRODUCTION

Lifting surfaces, as used in aircraft or wind turbines, are subjected to unsteady aerodynamic loads. Depending on the conditions of the flow and the characteristics of the supporting structure of the lifting surface, undesirable aeroelastic phenomena such as dynamic stall or stall flutter can occur. Methodologies to model such phenomena exist but are not universally applicable due to time of computation or accuracy. The main problem related to the modelling of stall flutter is the simulation of the unsteady aerodynamic phenomenon of dynamic stall. Current methods used to simulate unsteady aerodynamics make use of a steady integral boundary-layer solution coupled with an unsteady potential flow solution, such as [1] or more recently [2]. Usually, unsteady effects in the boundary layer are neglected, resulting in a reduction in fidelity. With the accurate calculation of unsteady aerodynamic loads it is possible to couple the fluid model to a mechanical model in order to solve for the motion of the lifting surface and hence simulate aeroelastic phenomena.

This paper presents a method that makes use of a 2D viscous-inviscid coupled method that consists of an unsteady interactive boundary layer model with the shedding of point vortex blobs. The inviscid problem is solved by means of a panel method, by the discretization of the airfoil into vortex panels and the wake into vortex blobs. The solution of the boundary layer equations is carried out using an adaptive finite volume scheme limited to the laminar section of the boundary layer. The boundary layer is solved at each time step in a time marching scheme, where the instantaneous edge velocity is imposed. This solution scheme has been developed as an extension of the method presented by Lloyd and Murman [3]. Viscous-inviscid coupling is performed through the imposition of a

permeation velocity to model the influence of the displacement thickness in the potential flow. Further interaction is considered with the addition of a free wake at each separation point and at each time step.

The present method was first introduced in [4] and was extended in [5]. The current paper continues the extension of the method to include the unsteady boundary-layer solution coupled with the effects of highly separated flows.

2 MODEL

The proposed model is composed of an inviscid solver coupled with a viscous solver, considering a wake formed by vortex blobs.

2.1 Inviscid Model

The inviscid flow equations are solved by superposing solutions of the Laplace equation. These solutions are linear and can be used to represent different aspects of the flow. The flow related to the airfoil surface is modelled using a vortex panel method. Source panels are added to consider the effects of the boundary-layer, as explained in subsection 2.3. The flow related to the wake is modelled using vortex blobs. This solution setup can be seen in figure 1.

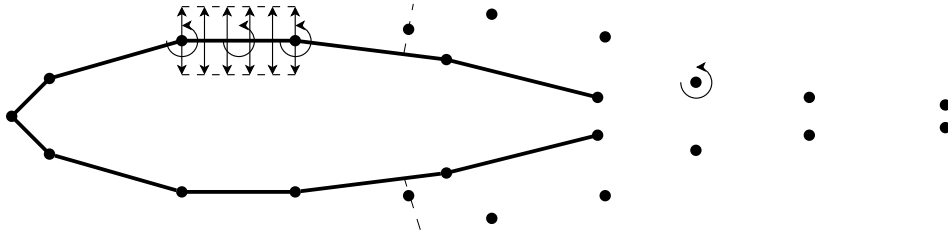


Figure 1: Aerodynamic model

The panel method is based on the distribution and superposition of vortices over a surface called a panel. In two dimensions, the method considers panels that have two boundary points and one collocation point. The boundary points determine the geometry of the panel. The collocation point is the point where the boundary conditions are imposed. The imposition of the boundary conditions determine the strength of the vortex panel.

The Kutta condition is imposed by specifying that the total vorticity at the trailing edge is zero. This approach ensures separation at the trailing edge and is discussed in detail by Katz and Plotkin[6].

To take into account the thickness of the trailing edge in the case where it is not zero, a constant strength source panel is added, as explained by Drela [7]. This panel is shown in figure 2.

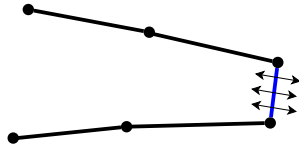


Figure 2: Trailing edge detail

2.2 Viscous Model

The viscous formulation is based on the solution of the unsteady boundary layer equation.

$$\frac{\partial u}{\partial x} + \frac{\partial v}{\partial y} = 0 \quad (1)$$

$$\frac{\partial u}{\partial t} + u \frac{\partial u}{\partial x} + v \frac{\partial u}{\partial y} = \frac{\partial u_e}{\partial t} + u_e \frac{\partial u_e}{\partial x} + \nu \frac{\partial^2 u}{\partial y^2} \quad (2)$$

This system of equations is discretized using a finite volume scheme. The scheme was first introduced for steady state in [3] and later extended to consider unsteady conditions in [5]. The equations are a nonlinear parabolic system. The system is solved at each station in direct mode and this solution is used to obtain the solution at the next station. The scheme is started at the stagnation point and advances station to station until the boundary layer solution is no longer obtainable. At each station, the equations are solved using a Newton-Raphson scheme.

$$Direct \Rightarrow \begin{cases} u(x, 0) = 0 \\ v(x, 0) = 0 \\ u(x, z_e) = u_e \end{cases} \quad (3)$$

The stability of the solution depends on the wall shear stress value. As the separation point is approached and the wall shear stress approaches zero, the solution might not be obtainable using the direct procedure. In this paper we propose a modified equation system to improve the stability and convergence of the solution in the presence of low wall shear stress. This can be achieved by extending the set of equations and considering the displacement thickness as part of the solution. From the definition of the displacement thickness, the following equation is obtained to calculate it

$$\delta^* = z_e - \frac{\psi_e}{\rho u_e} \quad (4)$$

The solution delivered by the algorithm can be seen in figure 3. In this case, we show the wall shear stress. The values from 0 to the dashed line are obtained using the direct mode with no modification of the equation system. At this point the solution no longer converges and the modified system is used. All results to the right of the dashed line are obtained using the modified system.

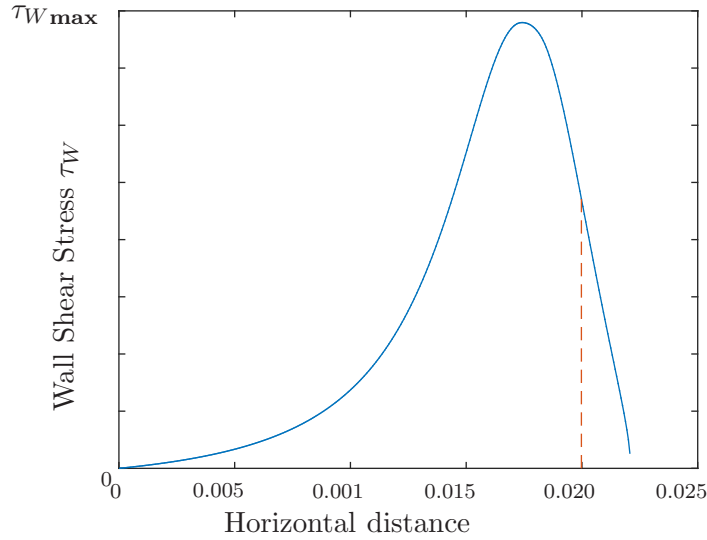


Figure 3: Algorithm separation. Dashed line divides between both methods

2.3 Viscous-Inviscid Interaction

In order to capture the effect of the presence of the boundary layer in the potential flow, a permeation velocity is considered in the panel method solution. The permeation velocity is a way of modelling an injection of air sufficient to displace the streamlines outwards by a distance equal to the displacement thickness from the surface of the airfoil. The displacement thickness is a measurement of the mass deficit in the potential flow due to the boundary layer, and the permeation velocity is equal to that deficit.

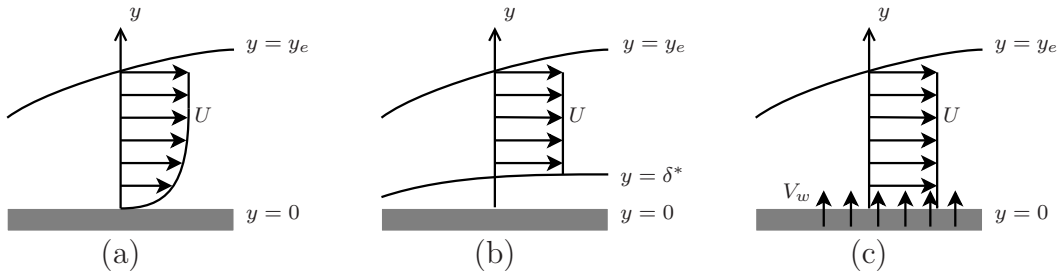


Figure 4: (a) Real flow, (b) flow modified using displacement thickness, (c) flow modified using permeation velocity

In figure 4 the model matching is presented. The real flow is the flow on the boundary layer without any modification. The displacement thickness can be used as a virtual surface on the airfoil that modifies the potential flow outside the boundary layer. The permeation velocity is equivalent to the displacement thickness addition. The formulation of the permeation velocity is related to the external velocity and the displacement thickness by

$$V_w = \frac{\partial}{\partial x} (U_e \cdot \delta^2) \quad (5)$$

The update of the external velocity U_e is carried out in a loop, as shown in figure 5.

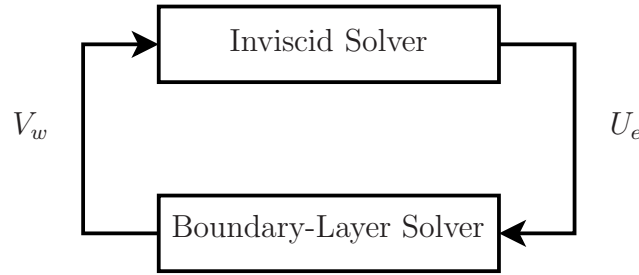


Figure 5: Update loop

2.4 Wake Model

The wake is modelled using point vortices that move with the local velocity. Considering that the velocity induced by a vortex diverges to infinity close to its center, the velocity field has to be modified. The solution used in this paper is the distribution of the vorticity over a certain area, as first introduced in [8], as opposed to having it concentrated in one point, which is the standard model for vortices.

The distributed vorticity can be calculated as a function of the radius from

$$\omega(r) = \Gamma e^{(-r^2/r_0^2)} \quad (6)$$

where r is the distance from the center of the vortex, r_0 is the radius of the circle in which the vorticity is distributed and Γ is the vortex strength.

The magnitude of the velocity induced by the vortex is modified as shown in figure 6.

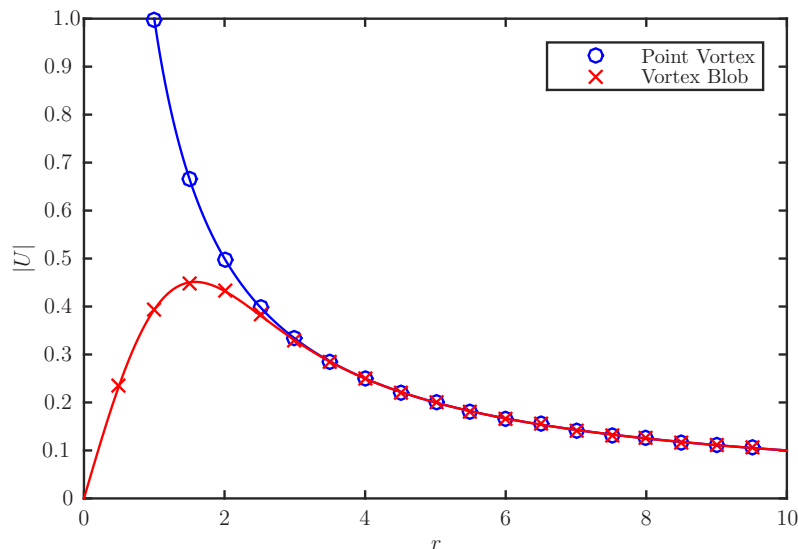


Figure 6: Velocity distribution induced by point vortex and vortex blob

The calculation of the strength of the vortices is carried out by taking into account the circulation present in the boundary layer. For a specific separated shear layer,

$$\Gamma = \int \gamma dA = \oint u dl \quad (7)$$

where Γ is the total circulation in the boundary-layer, γ is the circulation field in the boundary-layer, dA is the differential area of the boundary-layer and dl is the differential length of the curve that encloses the boundary layer.

This circulation yields two values, one for each separated shear layer (and, hence, wake). The strength of the newly shed vortices has to comply with Kelvin's circulation theorem, which states that in a potential flow, within a closed curve, the angular momentum is conserved in time.

$$\frac{\partial \Gamma}{\partial t} = 0 \quad (8)$$

In order to impose Kelvin's theorem, the the following equation is added to the panel method equation system

$$\int \gamma ds + a (\Gamma_{\text{Btm Skin}} + \Gamma_{\text{Top Skin}}) = - \sum \Gamma_{\text{Current}} \quad (9)$$

where Γ_{Current} is the total circulation that exists in the flow at the start of the current time step, γ is the circulation around the airfoil, a is a proportionality constant calculated at each timestep to fullfill Kelvin's theorem, $\Gamma_{\text{Btm Skin}}$ is the total circulation at the bottom boundary layer and $\Gamma_{\text{Top Skin}}$ is the total circulation at the top boundary layer.

2.5 Vortex convection

The propagation of the wake vortices is calculated using the local velocity and a third order Runge-Kutta scheme. This procedure is necessary to ensure that the motion of the vortices is reversible, which itself ensures that the trajectory is correct.

Considering for each time step 3 points

- \mathbf{x}_1 : at time $t = 0$
- \mathbf{x}_2 : at time $t = \Delta t/2$
- \mathbf{x}_3 : at time $t = \Delta t$

the propagation algorithm can be summarised as

1. Calculate the velocity \mathbf{u}_1 at point \mathbf{x}_1
2. Estimate a new position, $\mathbf{x}_2 = \mathbf{x}_1 + \mathbf{u}_1 \Delta t/2$
3. Calculate the velocity \mathbf{u}_2 at point \mathbf{x}_2
4. Estimate a new position, $\mathbf{x}_3 = \mathbf{x}_2 + \mathbf{u}_2 \Delta t/2$
5. Calculate the velocity \mathbf{u}_3 at point \mathbf{x}_3
6. The new position is calculated from $\mathbf{x}_3 = \mathbf{x}_1 + (\mathbf{u}_1 + 4\mathbf{u}_2 + \mathbf{u}_3)\Delta t/6$

2.6 Loads Calculation

The solution of the velocity field over the airfoil yields the local velocity, which is in turn used to calculate the potential on the skin. To calculate this potential, the velocity field is integrated, starting from the definition of the differential of the potential and using the relationships between u, v and Φ

$$d\Phi = \frac{\partial\Phi}{\partial x}dx + \frac{\partial\Phi}{\partial y}dy \quad (10)$$

$$d\Phi = udx + vdy \quad (11)$$

To integrate this function, a reference value must be chosen. In this case we consider a point upstream from the stagnation point follow it to the stagnation point. The path used to find the reference point is shown in figure (7).



Figure 7: Path used to integrate the potential Φ

Once the potential is calculate, the pressure is evaluated from the unsteady Bernoulli equation

$$\frac{p_\infty - p}{\rho} = \frac{1}{2} (u^2 + v^2) + \frac{\partial\Phi}{\partial t} \quad (12)$$

where p_∞ is reference pressure at infinity, p is the pressure on the collocation point of a panel and ρ is the fluid density. The pressure coefficient for each panel can be defined as

$$C_p = -\frac{u^2 + v^2}{U_\infty^2} - \frac{2}{U_\infty^2} \frac{\partial\Phi}{\partial t} \quad (13)$$

Finally, the total force on the airfoil is calculated from

$$\mathbf{F} = -\sum_{k=1}^{n_p} C_{p_k} \left(\frac{1}{2} \rho U_\infty^2 \right) \Delta S_k \mathbf{n}_k \quad (14)$$

where \mathbf{F} is total force on airfoil, C_{p_k} is the pressure coefficient on the k th panel, ΔS_k is the length of the k th panel and \mathbf{n}_k is a unit vector normal to the k th panel.

3 RESULTS

The performance of the complete numerical procedure is demonstrated on a 2D NACA 0012 airfoil, with a chord of $0.3[m]$. The flow speed is $25[m/s]$ and the angles of attack considered are 5° , 10° , 15° and 20° .

The airfoil is divided into 400 panels. This number is chosen to ensure a satisfactory coupling between the potential flow and the boundary layer solution. The boundary layer considered here has 350 elements in the x direction and 50 in the y direction. The size of the timestep is $0.02[s]$ and the blob radius chosen is $0.02[m]$.

3.1 Wake Dynamics

The results shown here are the shape of the wake for each selected angle of attack for two different time steps. The airfoil is initially at rest at the given angle of attack and an impulsive start is considered.

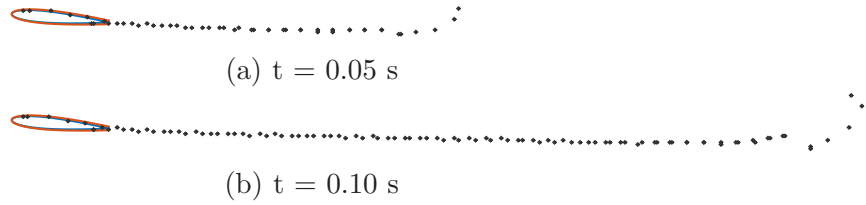


Figure 8: Wake shape 5°

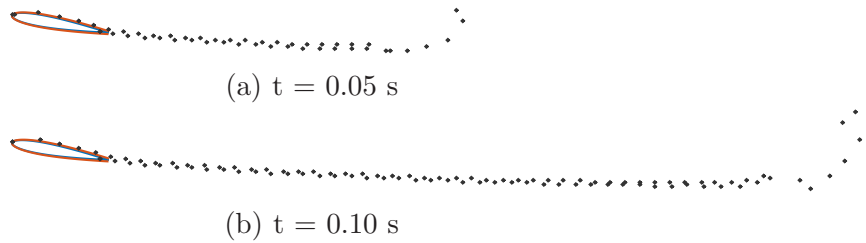


Figure 9: Wake shape 10°

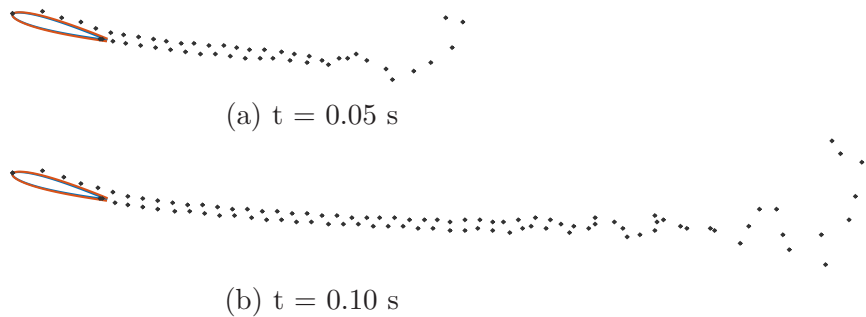
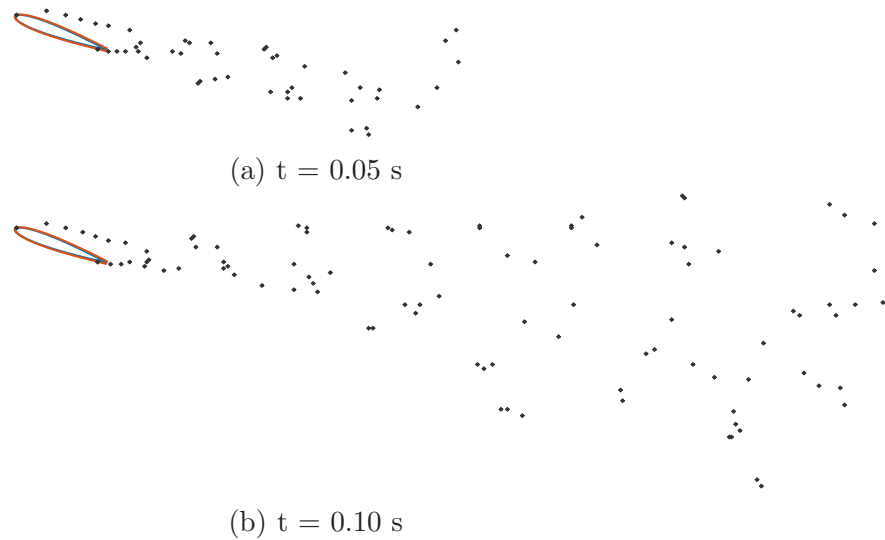


Figure 10: Wake shape 15°

The figures for 5° and 10° show a wake rollup that is consistent with what is to be expected with traditional attached flow models. For 15° some oscillations are observed as the vorticity in the upper separated shear layer becomes strong enough to interact with that of the lower. The wake shape for the 20° angle of attack shows high distortions as the flow on the upper side is fully separated and strong vortices propagate downstream. The interaction between the vortices from the two separated layers causes them to move away from each other; the vortex spread is limited by the choice of the vortex blob radius.

All the results show a separation point that might be considered too close to the leading edge. This can be explained by the high curvature around the leading edge that induces a locally abrupt velocity change that causes the wall shear stress to drop to zero. It should be kept in mind that the flow is fully laminar, therefore the separation is also laminar. The application of a turbulence model could modify the equation system in a way that forces the separation point to move further downstream.

Figure 11: Wake shape 20°

3.2 Aerodynamic Forces

The results here show the variation of the lift in time. All results are compared against the Wagner solution [9]. The potential flow solution is also indicated as a reference. Results are presented in figure 12

The figures for 5° , 10° and 15° show a behaviour similar to the one determined using Wagner's method. This compares well against experimental data as the flow is nearly attached and potential flow solutions are valid. The behaviour for 20° shows an unexpected initial reduction of the lift. This instantaneous downforce cannot be explained in a satisfactory manner at this point.

4 CONCLUSIONS

The interactive boundary layer method proposed here appears to be a useful tool for the solution of the boundary-layer equations and their coupling to an inviscid flow model.

The unsteady boundary-layer solution indicates that the unsteadiness of the boundary layer can not be overlooked, since it can change the instantaneous position of the separation point and the instantaneous strength of the wake vortices.

The wake shape and lift results show realistic behaviour (apart maybe from the 10° results), which hints that the method, given the correct calibration of its parameters, can be used successfully in an aeroelastic model.

5 FURTHER WORK

The work still to be done in this model, to achieve a working code that can be used in an aeroelastic model, is:

- Outline and carry out experiments to calibrate the model parameters, such as vortex blob diameter, panel number, etc.

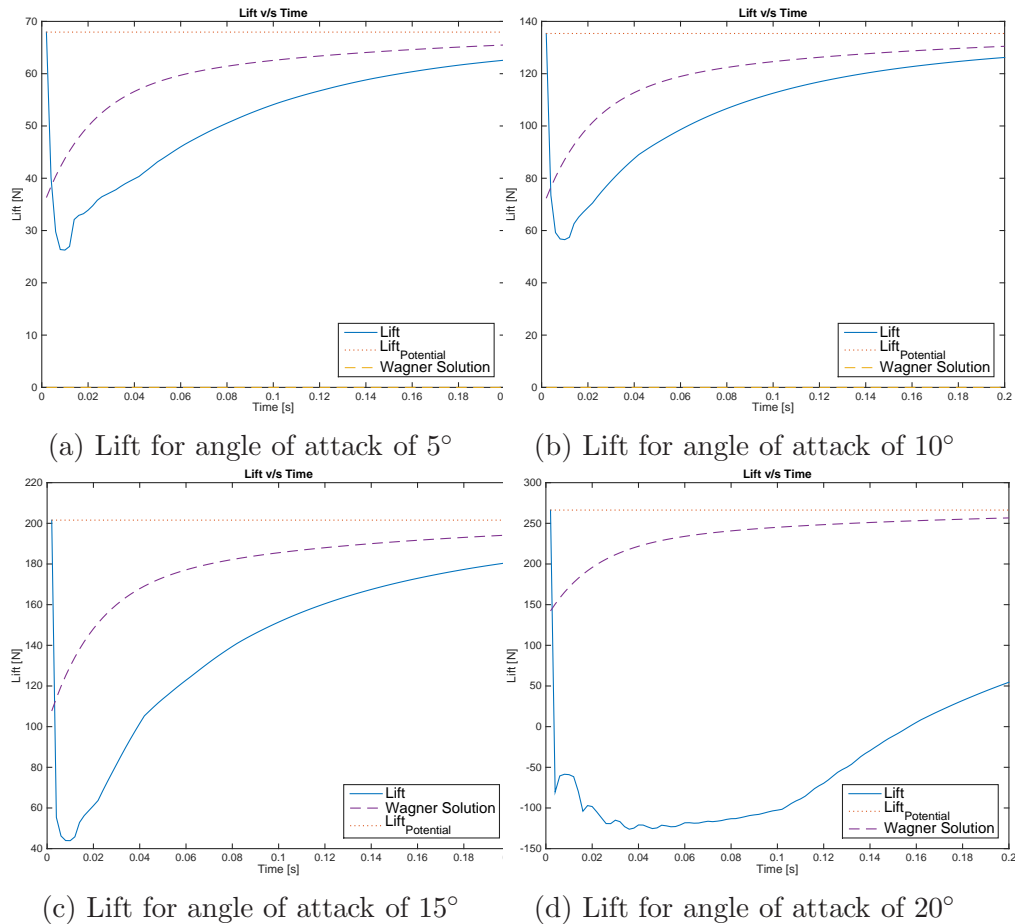


Figure 12: Lift acting on the airfoil at different angles of attack

- Wake shape and frequency to characterize the model accurately. This is to capture phenomena like Von Karman sheets if they are present.
- Study the extent and validity of the mixed viscous-inviscid coupling method for different Reynolds numbers.
- Carry out forced motion simulations, whereby the airfoil is forced to oscillate in pitch. Compare the results to experimental data from the literature.

6 REFERENCES

- [1] Riziotis, V. A. and Voutsinas, S. G. (2008). Dynamic stall modelling on airfoils based on strong viscous–inviscid interaction coupling. *International journal for numerical methods in fluids*.
- [2] Zanon, A., Giannattasio, P., and Simão Ferreira, C. J. (2013). A vortex panel model for the simulation of the wake flow past a vertical axis wind turbine in dynamic stall. *Wind Energy*.
- [3] B. Lloyd, E. M. (1986). Finite volume solution of the compressible boundary-layer equations. *NASA Contractor Report 4013*.

- [4] J. Rothkegel, G. D. (2011). Interactive boundary layer calculation of separated flows around 2d airfoils. *IFASD 2011*.
- [5] Rothkegel, J. I. and Dimitriadis, G. (2013). Dynamic stall and stall flutter simulations for a 2d airfoil using viscous-inviscid coupling. *Proceedings of the 54th AIAA/ASME/ASCE/AHS/ASC Structures, Structural Dynamics and Materials Conference*.
- [6] Katz, J. and Plotkin, A. (2001). Low-speed aerodynamics, vol. 13. Cambridge University Press.
- [7] Drela, M. (1989). Xfoil: An analysis and design system for low reynolds number airfoils. In *Low Reynolds number aerodynamics*. Springer, pp. 1–12.
- [8] Chorin, A. J. and Bernard, P. S. (1973). Discretization of a vortex sheet, with an example of roll-up. *Journal of Computational Physics*, 13(3), 423–429.
- [9] Wagner, H. (1925). Über die entstehung des dynamischen auftriebes von tragflügeln. *ZAMM-Journal of Applied Mathematics and Mechanics/Zeitschrift für Angewandte Mathematik und Mechanik*, 5(1), 17–35.

7 COPYRIGHT STATEMENT

The authors confirm that they, and/or their company or organization, hold copyright on all of the original material included in this paper. The authors also confirm that they have obtained permission, from the copyright holder of any third party material included in this paper, to publish it as part of their paper. The authors confirm that they give permission, or have obtained permission from the copyright holder of this paper, for the publication and distribution of this paper as part of the IFASD 2015 proceedings or as individual off-prints from the proceedings.